ORIGINAL ARTICLE

Photo-patternable and transparent films using cellulose nanofibers for stretchable origami electronics

Sangyoon Ji[1,4], Byung Gwan Hyun[1,4], Kukjoo Kim[1,4], Sang Yun Lee[2], Si-Hoon Kim[3], Ju-Young Kim[3], Myoung Hoon Song[2] and Jang-Ung Park[1]

Substantial progress in flexible or stretchable electronics over the past decade has extensively impacted various technologies such as wearable devices, displays and automotive electronics for smart cars. An important challenge is the reliability of these deformable devices under thermal stress. Different coefficients of thermal expansion (CTE) between plastic substrates and the device components, which include multiple inorganic layers of metals or ceramics, induce thermal stress in the devices during fabrication processes or long-term operations with repetitions of thermal cyclic loading–unloading, leading to device failure and reliability degradation. Here, we report an unconventional approach to form photo-patternable, transparent cellulose nanofiber (CNF) hybrid films as flexible and stretchable substrates to improve device reliability using simultaneous electrospinning and spraying. The electrospun polymeric backbones and sprayed CNF fillers enable the resulting hybrid structure to be photolithographically patternable as a negative photoresist and thermally and mechanically stable, presenting outstanding optical transparency and low CTE. We also formed stretchable origami substrates using the CNF hybrid that are composed of rigid support fixtures and elastomeric joints, exploiting the photo-patternability. A demonstration of transparent organic light-emitting diodes and touchscreen panels on the hybrid film suggests its potential for use in next-generation electronics.
NPG Asia Materials (2016) **8**, e299; doi:10.1038/am.2016.113; published online 26 August 2016

INTRODUCTION

Flexible or stretchable electronics are among the most attractive next-generation electronics in the foreseeable future owing to their various unprecedented possible applications,[1,2] such as in displays,[3,4] energy devices,[5] wearable electronics,[6,7] augmented or virtual reality devices,[8] smart living[9] and automotive electronics for smart cars.[10] In recent years, these deformable devices have been applied to diverse fields, and it has become increasingly important to improve their reliability against thermal stress. For example, automotive electronic devices are expected to function reliably in a temperature range from $-40\,°C$ (on a cold winter day) to $105\,°C$ (on a hot summer day).[11] In addition, the local temperature of displays or smartphones can rise above $60\,°C$ during operation. In contrast to rigid glass substrates with a low coefficient of thermal expansion (CTE <10 p.p.m. K^{-1}),[12] most plastic films for flexible electronics, such as polyethylene terephthalate (PET), polyimide (PI), polycarbonate (PC) and polyethylene naphthalate, have relatively high CTEs[13,14] exceeding 50 p.p.m. K^{-1}. The difference in CTE between plastic substrates and device components

that contain multiple inorganic layers of metals or ceramics induces thermal stress in the device region during thermal fabrication processing or device operation. Therefore, when deformable devices are exposed to environments with thermal cyclic loading–unloading or mechanical bending or stretching, the repetitions of residual stress can lead to fatigue failure.[15,16] Moreover, plastic substrates have relatively low mechanical strength and hardness, implying that they are limited in terms of safety-protecting devices. Furthermore, non-biodegradable plastic waste is generated from discarded devices, causing serious environmental concerns.[17,18] Therefore, there is a clear and urgent need for new substrate materials that support flexible or stretchable electronics.

Cellulose, the most abundant and biodegradable biomass in nature, has attracted tremendous interest as an alternative substrate material, especially in the form of nanofibers.[19,20] Individual singular nanofibers of cellulose exhibit low CTE, which is comparable to quartz glass, and an outstanding Young's modulus, which is higher than that of aluminum and glass fibers.[21,22] Although dense aggregates of cellulose

nanofibers (CNFs) can form flexible, transparent films for electronic devices,[23–26] there currently are still substantial challenges to the practical application of CNF films, such as (i) incompatibility with high-temperature processing ($<200\,°C$),[27] (ii) optical haze ($>20\%$ in visible light wavelengths)[28] derived from highly porous microstructures, (iii) poor water resistance ($<28°$ in water contact angle),[26,29] (iv) difficulty in forming complex, fine shapes and (v) limits in mechanical stretchability. To the best of our knowledge, the potential of CNF to provide stretchable but reliable electronic devices is yet unexplored. Here, we introduce a method to produce photo-patternable, transparent films that are flexible and also applicable as stretchable substrates supporting reliable devices, which are fabricated by electrospinning polymeric backbones and simultaneous spraying of CNF fillers. The resulting film can be patterned using photolithography as a negative photoresist, and this CNF hybrid structure can enhance thermal stability (thermal degradation temperature of 5% weight loss, $T_{5\%}$, at 280 °C), suppress light scattering (haze below 4% at 550 nm) and effectively increase water resistance (contact angle of 86°). This flexible CNF hybrid also shows excellent thermal (CTEs of 10 p.p.m. K^{-1}, similar to the glass case), optical (transmittance of 88% at 550 nm) and mechanical (Young's modulus of 5.5 GPa and tensile strength of 190 MPa, more than two times higher than those of polyimide or PET) properties and excellent reliability (negligible degradation in performance during a 10 000-cycle bending test and temperature–humidity bias test for 240 h in 85 °C and 85% relative humidity). Furthermore, exploiting its photo-patternability, reversible foldability and stretchability, origami forms of the substrate can be produced by integrating the CNF patterns with elastomeric joints. We demonstrate flexible touchscreen panels and transparent organic light-emitting diodes (TOLEDs) using a CNF hybrid film, providing evidence for its potential and widespread application in flexible and stretchable electronics. These remarkable functionalities, together with examples of practical applications, suggest a promising future for next-generation electronics.

EXPERIMENTAL PROCEDURES

Preparation of CNF hybrid film

2,2,6,6-tetramethyl-1-piperidine-1-oxyl-oxidized CNFs (0.3 wt%) ~ 20 nm in diameter and 1 µm long (University of Maine, Orono, ME, USA) were prepared for air-gun spray. For the electrospinning of epoxy nanofiber, SU-8 (Microchem, Inc.) and SU-8 thinner were mixed at a ratio of 10:1 (w/w). Afterward, the epoxy solution was loaded in a 1 ml plastic syringe attached to a syringe pump. The flow rate of the solution was 0.3 ml h^{-1}, and the inner diameter of the needle was 0.455 mm. During the electrospinning, high voltage (8.3 kV) was applied to the needle tip, and the copper collector was kept grounded. The distance between the needle tip and copper collector was ~ 15 cm. At the same time, as-prepared CNF solution was sprayed using an air-gun spray under applied pressure (30 p.s.i.). The volume of the CNF solution used in the spraying process was changed (100 ml, 200 ml and 300 ml). Next, obtained CNF–epoxy hybrid was annealed at 95 °C, which is the soft baking condition of epoxy, under pressure (10 MPa). Finally, the hybrid film was exposed to ultraviolet (UV) radiation for polymerization of SU-8 epoxy, and then the film was peeled off from the copper collector.

Characterization of CNF hybrid film

Optical transmittance with a 20-µm-thick hybrid film was measured with UV-vis-NIR (cary 5000, Agilent, Santa Clara, CA, USA). The transmittance was recorded every 0.5 nm throughout the spectrum range from 400 nm to 1500 nm. The mechanical analysis was performed using a micro UTM (Instron 5948, Norwood, MA, USA) for samples of 4 mm in length and 1 mm in width at a strain rate of 4 µm min^{-1}. Thermogravimetric analysis measurements were carried out using an SDT Q600 (TA Instruments, Leatherhead, UK) on samples of ~ 10 mg. Each sample was scanned over a temperature range from room

temperature to 600 °C. A CTE was evaluated by using a TMA (EXSTAR TMA/SS 6100, Seiko Instruments, Inc., Chiba, Japan) for a sample size of 10 mm in length and 2 mm in width from room temperature to 150 °C.

Fabrication of flexible touchscreen panel

The electrode layer was prepared by spin-coating the AgNW (Nanopyxis), which was dispersed in deionized water, onto hybrid film. The optical transmittance of this electrode layer was characterized in the same manner as described before. The flexibility (folding capability) of the electrode layer wrapped on various cylindrical supports with different curvatures was investigated using a probe station (Keithley 4200-SCS, Cleveland, OH, USA). Ten thousand cycles of a bending cyclic test at a bending radius of 0.5 mm with a frequency of 0.5 Hz were conducted by using a step motor controller (ECOPIA, Anyang, Korea). After coating the electrodes, the dot spacers consisting of polymer were photolithographically fabricated, and Au interconnects (50 nm) were deposited using a thermal evaporator. Finally, the upper and lower panels were carefully assembled and connected to the IC board (Touchdisplay, Co., Ltd, Seoul, Korea) and a desktop computer.

Fabrication of TOLED

The bottom electrode of poly(3,4-ethylenedioxythiophene):poly(styrenesulfonic acid) (PEDOT:PSS) (PH1000, Clevios, Hanau, Germany) doped with dimethyl sulfoxide (5 wt%) and Zonyl FS-300 (0.5 wt%) (PDZ) was spin-coated at 3000 r.p.m. for 45 s onto 50-µm-thick hybrid film and annealed at 115 °C for 10 min. A hole transport layer, PEDOT:PSS (AI 4083, Clevios), was spin-coated at 5000 r.p.m. for 45 s onto PDZ and was annealed at 145 °C for 10 min. Super yellow (Merck Co., Darmstadt, Germany, Mw = 1950 000 g mol^{-1}) solution dissolved in chlorobenzene (6.2 mg ml^{-1}) was spin-coated at 2000 r.p.m. for 45 s onto PEDOT:PSS layer for the emissive layer. And next, poly((9,9-bis(3′-(N,N-dimethylamino)propyl)-2,7-fluorene)-alt-2,7-(9,9–ioctylfluorene)) (PFN) (1-Material Co., Dorval, QC, Canada) was dissolved in methanol (0.1 wt%) and acetic acid (0.002 wt%) was spin-coated at 5000 r.p.m. for 45 s onto super yellow and was annealed at 110 °C for 10 min. Before deposition of top electrode, ZnO NP (Sigma Aldrich, St Louis, MO, USA) dissolved in isopropyl alcohol (IPA) (50 mg ml^{-1}) was spin-coated at 2000 r.p.m. for 45 s onto PFN as filler. Finally, for AgNW spray coating, the spray nozzle was positioned 80 mm above the substrate. The AgNWs (Nanopyxis, Jeonju, Korea) dispersed in IPA (0.25 wt%) were spray-coated onto PFN. The optical transmittance of the OLED was measured in the same manner as described before. For the TOLED, the J–V–L characteristics and device performance were measured using a spectroradiometer (CS-2000, Konica Minolta, Osaka, Japan) and a source meter (2400, Keithley), respectively.

Fabrication of stretchable origami substrates

A simultaneously deposited CNF–epoxy hybrid sample was soft-baked at 95 °C for 10 min under a pressure of 10 MPa. This soft-baked hybrid film was then selectively exposed to ultraviolet light using a photomask for 60 s to polymerize the SU-8 epoxy, followed by post-exposure baking at 95 °C for 5 min. Next, the hybrid film was developed by soaking in development solution and thoroughly rinsed using IPA. To fabricate a stretchable origami substrate, polydimethylsiloxane was spin-coated onto patterned hybrid film with a thickness of 100 µm and cured at 120 °C for 4 h. The stretchability of the origami substrate was evaluated using a motor controller (ECOPIA) and four-point measurement using a probe station (Keithley 4200-SCS).

RESULTS AND DISCUSSION

Preparation of the CNF hybrid film

Figure 1a schematically illustrates the manufacturing process for a CNF hybrid film. The three-dimensional web-like structure of epoxy was obtained by electrospinning, and the CNFs dispersed in deionized water (0.3 wt%) were sprayed simultaneously. As shown in Figure 1b, the three-dimensional nanoweb structure, which consists of electrospun epoxy nanofibers with an average diameter of 420 nm, has many pores (Supplementary Figure S1). This microporous structure of the epoxy nanoweb makes it difficult to form a uniform CNF–epoxy
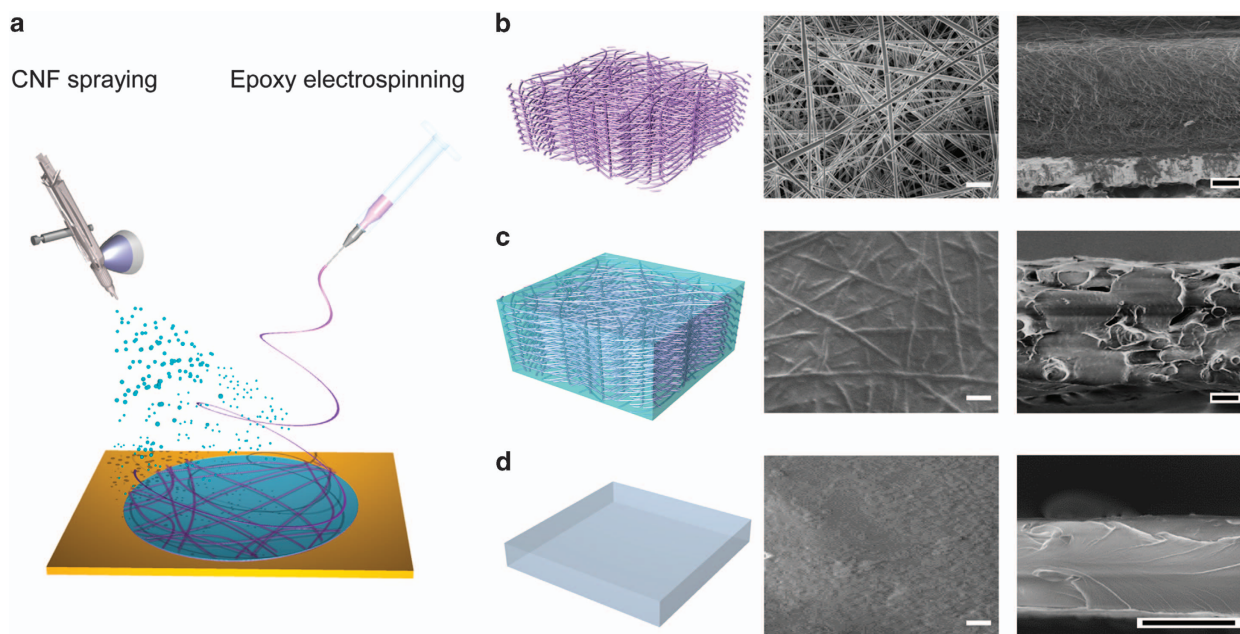
Figure 1 Preparation of the CNF hybrid film. (**a**) A schematic image of an electrospinning epoxy backbone and spraying CNF fillers simultaneously. Schematics and scanning electron microscopy (SEM) images (top and cross-sectional views) of (**b**) the electrospun three-dimensional (3D) epoxy nanoweb structure, (**c**) the CNF–epoxy hybrid before hot pressing and (**d**) the CNF–epoxy hybrid after hot pressing. White scale bars are 10 μm, and black scale bars are 20 μm.

composite using conventional coating methods such as dip-coating, spin-coating and vacuum filtration because it is difficult to impregnate several micron-long CNFs into the epoxy nanoweb structure. Therefore, an unconventional approach using simultaneous electrospinning and spraying is adopted for the formation of a uniform CNF–epoxy hybrid, which consists of a three-dimensional epoxy web filled with CNFs, as shown in Figure 1c. As the volume of sprayed CNF solution increases, the CNF–epoxy hybrid becomes denser with a high packing density (Supplementary Figure S2). However, the CNF–epoxy hybrid film still has a porous structure and a rough surface; therefore, we applied hot pressing, which is an effective way to improve the surface roughness[30] and remove residual pores by melting the electrospun epoxy nanofibers. For this hot pressing, the hybrid sample was annealed at 95 °C for 10 min under a pressure of 10 MPa. In our system, a 20-μm-thick, flexible and transparent CNF hybrid film with a highly densified structure and a smooth surface morphology (root-mean-square roughness: 0.7 nm) was obtained by spraying 300 ml of the CNF solution and sequential hot pressing, as shown in Figure 1d and Supplementary Figure S3. The film thickness can be controlled by modifying the electrospinning and spraying time (Supplementary Figure S4).

Optical, mechanical and thermal characteristics of the CNF hybrid film

We characterized the optical, mechanical and thermal properties of the hybrid films, which are the critical determinants of a substrate for electronic devices. Figure 2a shows photographs of a pristine epoxy film (spin-coated), a pristine CNF film (vacuum filtered) and a hybrid film. As shown in Figure 2b and Supplementary Figure S5, this pristine epoxy film exhibits an optical transmittance of 90% and haze of 3% (at 550 nm), whereas the CNF film has relatively low transmittance (77%) and high haze (18%) due to light scattering caused by the cavities and the rough surface of the film.[31] The hybrid film (volume

of the sprayed CNF solution: 300 ml), meanwhile, shows significantly improved optical properties (for example, transmittance of 88% and haze of 4%) compared with the pristine CNF film, indicating that the light scattering is significantly reduced because of the densely packed structure and reduced cavities within the hybrid structure. The mechanical property of each film is also characterized and described in the stress–strain curves in Figure 2c. The pristine CNF film has Young's modulus and tensile strength of 6 GPa and 220 MPa, whereas those of the epoxy film are 1.7 GPa and 40 MPa, respectively. Their hybrid structure, however, shows improved Young's modulus and tensile strength compared with the pristine epoxy film. In addition, as the volume of sprayed CNF solution increases, the hybrid film exhibits significantly enhanced mechanical properties. Young's modulus and tensile strength of the hybrid film formed by spraying 300 ml of the CNF solution are 5.5 GPa and 190 MPa, respectively, which are three times higher than those of the epoxy film. These enhanced mechanical properties can be attributed to the reinforcing effect of the high-strength CNFs in the hybrid film and are superior to those of commonly used plastic substrates. Young's moduli of PET and polyimide are 2 GPa and 2.5 GPa, respectively.

In addition to the optical and mechanical performances, thermal stability is another important factor of a substrate. A large difference in CTEs between the substrate and other layers of devices causes undesirable stress at the interface, thereby leading to the bending or distortion of the whole device during the fabrication process, which typically involves high-temperature treatments. A low CTE value, typically < 20 p.p.m. K^{-1}, is required to match the thermal expansion of the substrate to that of other layers of thin-film electronic devices.[15] However, commonly used plastic substrates, such as PET and polyimide, have relatively high CTE values > 50 p.p.m. K^{-1}. As shown in Figure 2d, the CTE of the epoxy film (53 p.p.m. K^{-1}) is also too high to be utilized as a substrate for thin-film electronic devices. Conversely, the hybrid film formed by spraying 300 ml of the CNF
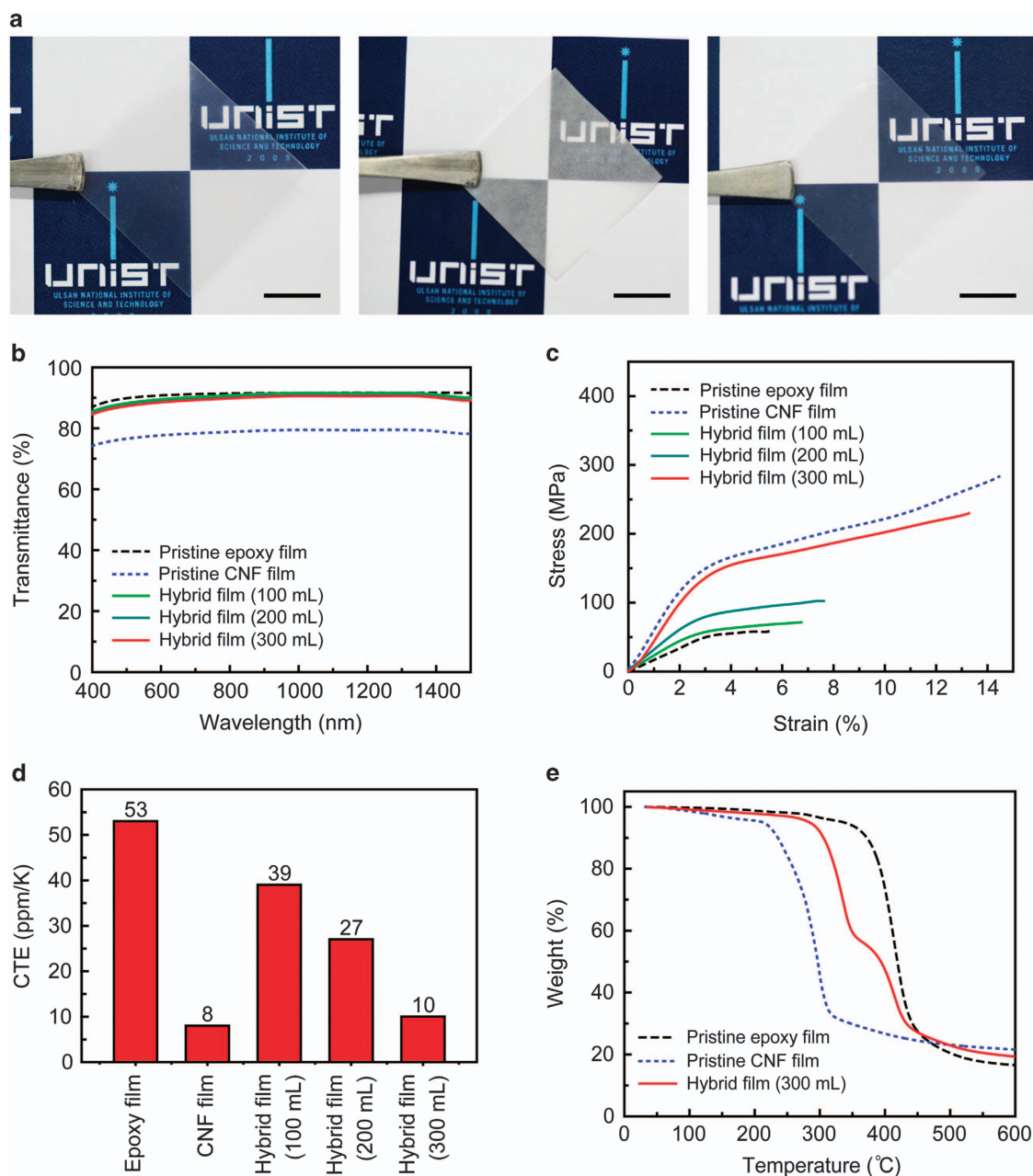
Figure 2 Optical, mechanical and thermal characteristics of the CNF hybrid film. (**a**) Photographs of a pristine epoxy film (spin-coated, left), a pristine CNF film (vacuum filtered, middle) and a hybrid film (right). Scale bars, 1 cm. (**b**) Optical transmittance spectra of each film in the range from 400 nm to 1500 nm. (**c**) Stress–strain curves for each film. The hybrid shows significantly enhanced mechanical properties compared with pristine epoxy film. (**d**) Coefficient of thermal expansion of each film. (**e**) Thermogravimetric analysis (TGA) shows the weight change of each film as a function of temperature. The hybrid film remains stable up to 280 °C.

solution shows a significantly reduced CTE (10 p.p.m. K^{-1}) because the thermal stress in the epoxy is largely suppressed by the CNF network. The temperature–humidity bias test was also conducted to examine the thermal/chemical reliability of this hybrid film. To examine the sole effect of the CTE value (thermal expansion) of the substrates on the mechanical failure of the electrode materials, other variables, such as an instability in oxidation, which may influence the test results, should be excluded. Therefore, as an example, a chemical vapor deposition-synthesized graphene layer, which is stable against thermal oxidation, was transferred onto a PET film or this hybrid film

and then exposed to the conditions of 85 °C and 85% relative humidity for 240 h. The graphene on the PET film shows significant changes in the sheet resistance (R_s) of graphene because large thermal expansion of the PET substrate (~60 p.p.m. K^{-1}) (Supplementary Figure S6) induces cracks in the graphene layer. In contrast, the R_s of graphene changes negligibly on the hybrid film owing to the low thermal expansion of the hybrid film, indicating that this hybrid film with the low CTE can be compatible with other functional layers of devices. Figure 2e and Supplementary Figure S7 present the thermogravimetric analysis results showing the weight loss of each film as a
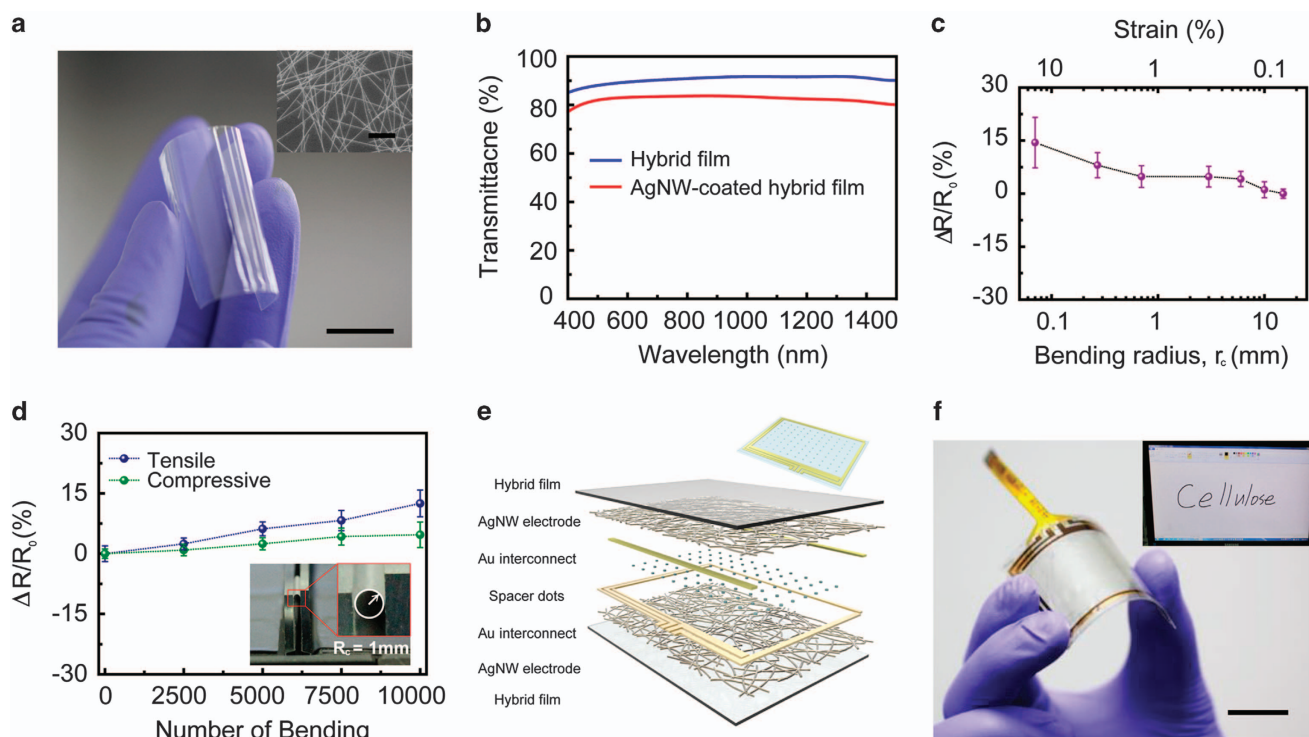
Figure 3 Flexible touchscreen panel using hybrid film. (**a**) Photographs of the AgNW-coated hybrid film. Scale bar, 2 cm. The inset shows an scanning electron microscopy image of uniformly coated AgNW electrode on the hybrid film. Scale bar, 2 μm. (**b**) Optical transmittance spectra of the hybrid film and AgNW-coated hybrid film. (**c**) Relative resistance changes of the AgNW electrode on the hybrid film as a function of bending radius and bending-induced strain. (**d**) Cyclic bending fatigue test of the AgNW electrode on the hybrid film for 10 000 cycles at a bending radius of 0.5 mm. (**e**) A schematic structure and (**f**) a photograph of the touchscreen panel fabricated on the hybrid film. Scale bar, 2 cm. The inset and Supplementary Movie S1 show the operation of the touchscreen panel.

function of temperature. The CNF and the epoxy film exhibit a single-stage degradation peak of 5% of the weight loss ($T_{5\%}$) at 216 and 336 °C, respectively, whereas the hybrid film with the largest CNF concentration shows two distinct degradation peaks. The first stage begins at 280 °C, which mainly involves the thermal degradation of the CNFs, and the second stage, which starts at 356 °C, involves the thermal degradation of the epoxy. The thermal decomposition of the hybrid film occurs at a higher temperature than the pristine CNF film owing to the epoxy barrier, which retards oxygen permeation and rapid heat transfer within the hybrid film.

Demonstration of a flexible touchscreen panel using the hybrid film
As an example of the application of the hybrid film, we demonstrate here a four-wire resistive touchscreen panel utilizing hybrid films as substrates for both sides of the touchscreen panel with transparent electrodes of silver nanowire (AgNW) random networks. Typically, a pristine cellulose film is vulnerable to water[29] and, therefore, is incompatible with water-based solution processes. The hybrid film, however, shows an increased contact angle of the film from 42° to 86°, indicating that the remaining epoxy enhances the hydrophobicity of the hybrid (Supplementary Figure S8). This improved water resistance improves the process capabilities of the hybrid films. Figure 3a shows a photograph of this AgNW-coated, 20-μm-thick hybrid film, and the inset scanning electron microscopy image presents a uniformly coated AgNW electrode on the hybrid film. The optical transmittance of this sample (including the hybrid substrate and AgNWs) is 83% (at 550 nm), indicating that ~4–5% loss of transmittance is introduced by the AgNW electrode (Figure 3b). This AgNW electrode on

the hybrid film shows excellent mechanical flexibility, as shown in Figures 3c and d. Figure 3c shows the relative change in resistance ($\Delta R/R_0$) as a function of the bending radius (R_c). The resistance of the electrode is negligibly changed even at a bending radius as small as 270 μm. It then slightly increases by 12% upon bending with a radius < 100 μm, implying that the AgNW network is damaged at a bending-induced strain (ε) of 10% (see Supplementary Information). The mechanical reliability was further investigated by a cyclic bending test (10 000 cycles) with a radius and frequency of 0.5 mm and 0.5 Hz, respectively. As plotted in Figure 3d, the R_s of the AgNW electrode (initial $R_s = 12\,\Omega\,\mathrm{sq}^{-1}$) slightly increases by 11 and 5% during the repetitive tensile and compressive bending (10 000 cycles), respectively. These AgNW-coated hybrid films are utilized as substrates for the touchscreen panel, as illustrated in Figure 3e. The polymer dot spacers and gold interconnects (50 nm thick) are patterned on the AgNW-coated hybrid substrate by photolithography and metal evaporation. Subsequently, the upper and lower panels are assembled and connected to a controller circuit and a desktop computer. Figure 3f and Supplementary Movie S1 show the operation of the transparent and flexible touchscreen panel fabricated on the hybrid substrates. To characterize the thermal stability of integrated touchscreen panels (TSPs), TSPs with different substrates (CNF hybrid films and PET films) were exposed to temperature of 100 °C for 10 days. The TSP using hybrid films was operated stably, and no cracking on the gold interconnections was observed after 10 days. Conversely, the TSP using PET films did not operate normally because thermal expansion of the PET film caused many cracks on the gold interconnections (Supplementary Figure S9). This stable operation
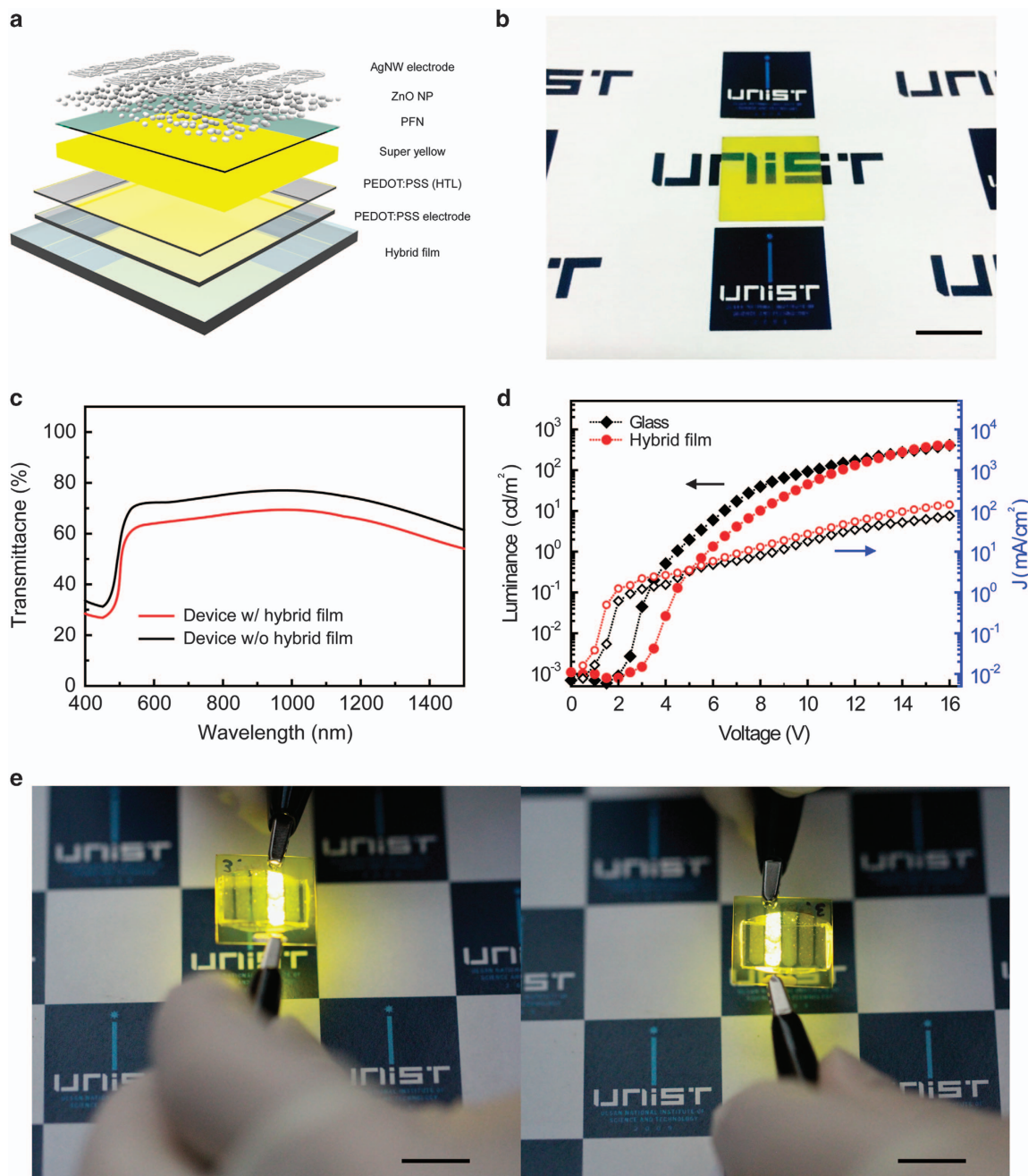
Figure 4 Transparent OLED (TOLED) on the hybrid film. (**a**) Schematic structure of the TOLED on the hybrid film. (**b**) Photograph of the TOLED device with high transparency. Scale bar, 1 cm. (**c**) Optical transmittance spectra of the TOLED device including and excluding the substrate transmittance. (**d**) Comparison of current density versus applied voltage and luminance versus applied voltage curves of the TOLED on the hybrid film and the glass. (**e**) Photographs of the TOLED on the hybrid substrate emitting light through both top and bottom directions. Scale bars, 1 cm.

of the TSP with the CNF hybrid substrate can be attributed to the minimized mismatch of CTEs between the metal electrodes (CTE ~ 14 p.p.m. K^{-1}) and our CNF hybrid films (CTE of 10 p.p.m. K^{-1}).

Demonstration of a transparent OLED on the hybrid film

The hybrid film can also be used as a flexible substrate for TOLEDs, suggesting a promising strategy towards next-generation transparent displays. Figure 4a illustrates a schematic diagram of the device structure. The TOLED on the 50-μm-thick hybrid film is composed of (PEDOT:PSS) doped with dimethyl sulfoxide and zonyl fluorosurfactant (PDZ) as a transparent anode,[32] PEDOT:PSS as a hole

transport layer, super yellow as an emitting layer, PFN as an electron-injection layer and zinc oxide nanoparticles (ZnO NPs)/ AgNWs as a transparent cathode. The large openings within the AgNW network cathode are likely to induce a non-uniform electrical field distribution,[33] which is undesirable for the stable operation of OLEDs. Therefore, ZnO NPs were employed as filler materials, and the resulting ZnO NP/AgNW layer can work as the cathode in the device.[34] All layers were formed via solution processes (that is, spin-coating and spray coating) without any vacuum process. Figure 4b shows a photograph of the TOLED on the hybrid substrate. The TOLED shows high transparency so that the background letters could
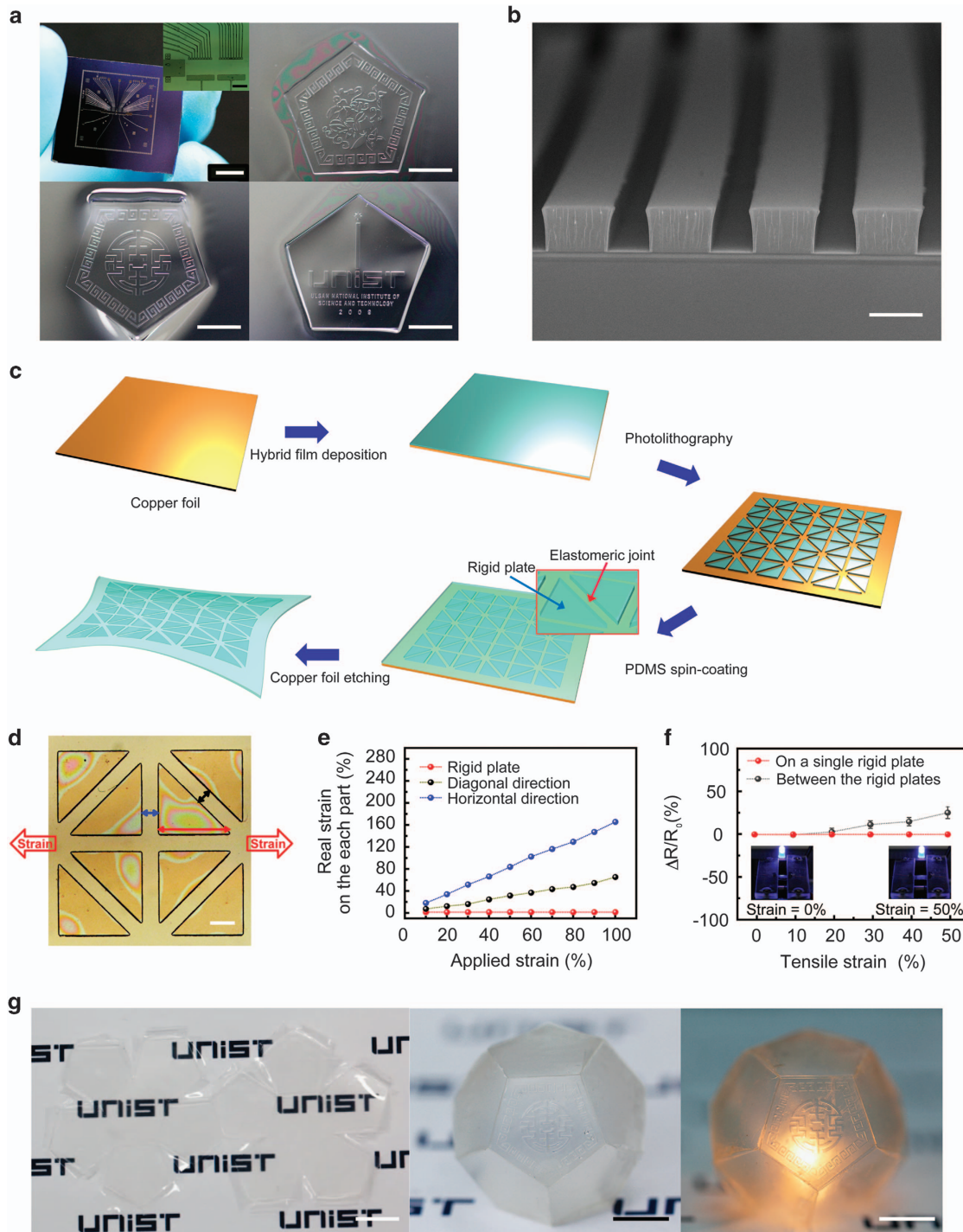
Figure 5 Fabrication of the reversibly foldable and stretchable substrate for stretchable origami electronics. (**a**) Photographs and optical micrographs of various patterns (an electronic circuit, letters, a Korean traditional symbol and a lotus) of the hybrid film. Scale bars, 5 mm. (**b**) 50 μm-thick CNF hybrid film patterned with an aspect ratio higher than 1:1 and feature size of 50 μm. Scale bar, 50 μm. (**c**) Schematic illustration of the fabrication process for the stretchable origami substrate by patterning the CNF hybrid into the isosceles right-angled triangle rigid plates, followed by spin-coating of polydimethylsiloxane (PDMS) elastomer. (**d**) Optical micrograph of the fabricated stretchable origami substrate. Scale bar, 200 μm. (**e**) Effective strains on each part along the direction indicated by colored arrows in **d**. (**f**) Relative changes in the resistance of the AgNW electrode coated on the stretchable origami substrate under various tensile strains. Inset images indicate that the blue inorganic light-emitting diode (ILED) still illuminates upon 50% tensile strain of the substrate. (**g**) A planar figure for the origami structure made of the stretchable origami substrate and its completed origami structure. The right image demonstrates the illumination of an inorganic light-emitting diode inside the regular dodecahedron origami structure. All scale bars (white and black), 1 mm.

8

be clearly recognized. The optical transmittance of the TOLED including and excluding this hybrid substrate at 550 nm were 62 and 70%, respectively, as shown in Figure 4c. The device performance was evaluated by the current density versus the applied voltage (J–V) and the luminance versus the applied voltage (L–V). As shown in Figure 4d, the TOLED fabricated on the hybrid film presented a maximum luminance of 410.3 cd m^{-2}, which is comparable to the luminance of 442.7 cd m^{-2} of the TOLED fabricated on the glass. The detailed performance of fabricated TOLEDs, including luminous efficiency, power efficiency, external quantum efficiency and emitting spectrum, are shown in Supplementary Figure S10. Figure 4e and Supplementary Movie S2 show the stable operation of the TOLED fabricated on the hybrid substrate, emitting light through both the top and bottom directions.

Reversibly foldable and stretchable substrate for stretchable origami electronics

The evolution of electronics has increased consumer demand for electronic devices with various form factors, which ultimately require a substrate that is patternable and deformable in arbitrary shapes. To achieve this functionality, we suggest a patternable and foldable substrate using our CNF hybrid film. Although many previous studies have reported on stretchable interconnects using graphene,[35] metal nanowires,[36] metal nanofiber,[37,38] and geometrical approaches,[39] conventional electronic devices fabricated on the elastomeric substrate are easily broken because most of the semiconductor, dielectric and encapsulation materials are still brittle. Therefore, the approach using origami substrates made of strain-free rigid plates with reversibly foldable and stretchable, elastomeric joints[40] has been considered as a promising strategy for stretchable electronics. Our hybrid film with outstanding mechanical, optical and thermal properties can also be used for the origami substrates by imparting photo-patternability to the CNF hybrid. The CNF hybrid can be patterned as a negative photoresist. Figure 5a shows photographs and optical micrographs of various patterns (that is, an electronic circuit, letters, a Korean traditional symbol and a lotus) of the hybrid. As shown in Figure 5b, the 50-μm-thick hybrid film can be patterned into the structure with an aspect ratio higher than 1:1 and a feature size of 50 μm. A stretchable origami substrate was fabricated by patterning the hybrid film into isosceles right-angled triangle rigid plates, followed by spin-coating of polydimethylsiloxane elastomer with a thickness of 100 μm, as shown in Figures 5c and d. Figure 5e plots the effective tensile strain on each part, as indicated by the colored arrows in Figure 5d, ($\varepsilon_{horizontal}$: strain along the horizontal direction; $\varepsilon_{diagonal}$: strain along the diagonal direction; ε_{plate}: strain on the rigid plates), when a tensile strain (ε) is applied to the stretchable origami substrate. Whereas the elastomeric soft region in the substrate absorbs large effective strains ($\varepsilon_{horizontal} = 1.62\ \varepsilon$, $\varepsilon_{diagonal} = 0.59\ \varepsilon$), the rigid plates composed of the patterned CNF hybrid experience negligible strains regardless of the applied strain ($\varepsilon_{plate} = 0$). The relative changes in the resistance of the AgNW electrode coated on this substrate under various tensile strains is plotted in Figure 5f. During the stretching of up to 50%, the resistance of the electrode on a single rigid plate remains almost constant, and the resistance of the electrode on the elastomeric joint between the rigid plates was slightly changed ($\Delta R/R_0 = 24\%$ at a strain of 50%), which is still acceptable as an electrode by considering the low initial resistance ($R_0 = 13\ \Omega$). This stretchable origami substrate with structural uniqueness can also be utilized as a foldable substrate for emerging origami electronics. An origami

geometry fabricated by folding the AgNW-coated hybrid substrate was used as an interconnect for an inorganic light-emitting diode, as shown in Figure 5g. The left and middle images in Figure 5g show the planar figure for the origami structure made of the foldable, CNF hybrid substrate and its completed origami structure, respectively. The right image in Figure 5g demonstrates the illumination of an inorganic light-emitting diode inside the regular dodecahedron origami structure, representing an aesthetic application example of the photo-patternable hybrid film.

CONCLUSION

In summary, we demonstrate a photo-patternable and transparent CNF hybrid film that is a flexible or stretchable substrate with superb mechanical, optical and thermal properties. The CNF with high Young's modulus and low CTE enhances the mechanical and thermal characteristics of this hybrid film. In addition, the epoxy with photo-patternability and hydrophobicity enables new functionality and effectively compensates for the drawbacks of the cellulose. The application examples demonstrated here (that is, a transparent and flexible touchscreen panel, a transparent OLED and photo-patternable substrates for origami electronics) represent unprecedented opportunities for various potential applications and provide a promising strategy for developing next-generation wearable electronics.

CONFLICT OF INTEREST

The authors declare no conflict of interest.

1 Forrest, S. R. The path to ubiquitous and low-cost organic electronic appliances on plastic. *Nature* **428**, 911–918 (2004).
2 Gates, B. D. Flexible electronics. *Science* **323**, 1566–1567 (2009).
3 Rogers, J. A., Bao, Z., Dodabalapur, A., Crone, B., Raju, V. R., Kuck, V., Katz, H., Amundson, K., Ewing, J. & Drzaic, P. Paper-like electronic displays: large-area rubberstamped plastic sheets of electronics and microencapsulated electrophoretic inks. *Proc. Natl Acad. Sci. USA* **98**, 4835–4840 (2001).
4 White, M. S., Kaltenbrunner, M., Głowacki, E. D., Gutnichenko, K., Kettlgruber, G., Graz, I., Aazou, S., Ulbricht, C., Egbe, D. A. M., Miron, M. C., Major, Z., Scharber, M. C., Sekitani, T., Someya, T., Bauer, S. & Saricifci, N. S. Ultrathin, highly flexible and stretchable PLEDs. *Nat. Photonics* **7**, 811–816 (2013).

Cellulose hybrid film for stretchable electronics
S Ji *et al*

9

5 Hu, L., Pasta, M., La Mantia, F., Cui, L. F., Jeong, S., Deshazer, H. D., Choi, J. W., Han, S. M. & Cui, Y. Stretchable, porous, and conductive energy textiles. *Nano Lett.* **10**, 708–714 (2010).

6 Park, Y. J., Lee, S.-K., Kim, M.-S., Kim, H. & Ahn, J.-H. Graphene-based conformal devices. *ACS Nano* **8**, 7655–7662 (2014).

7 Park, M., Park, Y. J., Chen, X., Park, Y.-K., Kim, M.-S. & Ahn, J.-H. MoS_2-based tactile sensor for electronic skin applications. *Adv. Mater.* **28**, 2556–2562 (2016).

8 Farandos, N. M., Yetisen, A. K., Monteiro, M. J., Lowe, C. R. & Yun, S. H. Smart lenses: contact lens sensors in ocular diagnostics (Adv. Healthcare Mater. 6/2015). *Adv. Healthc. Mater.* **4**, 785–785 (2015).

9 Gershenfeld, N., Krikorian, R. & Cohen, D. The internet of things. *Sci. Am.* **291**, 76–81 (2004).

10 Matsuzaki, R. & Todoroki, A. Wireless monitoring of automobile tires for intelligent tires. *Sensors* **8**, 8123–8138 (2008).

11 Mccluskey, P. & Nathan, K. Evaluating the performance and reliability of embedded computer systems for use in industrial and automotive temperature ranges. *CALCE Electron. Prod. Syst. Cent. Univ. Md.* **1**, 62–65 (2001).

12 Lin, Y. J., Hsieh, C. C., Yu, C. H., Tung, C. H. & Yu, D. C. H. Study of the thermo-mechanical behavior of glass interposer for flip chip packaging applications. In *Electron. Compon. Technol. Conf. ECTC 2011 IEEE 61st* 634–638, doi:10.1109/ECTC.2011.5898579 (2011).

13 Choi, M.-C., Kim, Y. & Ha, C.-S. Polymers for flexible displays: from material selection to device applications. *Prog. Polym. Sci.* **33**, 581–630 (2008).

14 Chen, Y., Mei, Y., Kaltofen, R., Mönch, J.I., Schumann, J., Freudenberger, J., Klauß, H. & Schmidt, O. G. Towards flexible magnetoelectronics: buffer-enhanced and mechanically tunable GMR of Co/Cu multilayers on plastic substrates. *Adv. Mater.* **20**, 3224–3228 (2008).

15 MacDonald, W. A. Engineered films for display technologies. *J. Mater. Chem.* **14**, 4–10 (2004).

16 Crawford, G. P. in *Flexible Flat Panel Displays* (ed. Crawford G. P.) (John Wiley & Sons, Ltd, 2005).

17 Liu, Q., Cao, J., Li, K. Q., Miao, X. H., Li, G., Fan, F. Y. & Zhao, Y. C. Chromosomal aberrations and DNA damage in human populations exposed to the processing of electronics waste. *Environ. Sci. Pollut. Res. Int.* **16**, 329–338 (2009).

18 Musson, S. E., Vann, K. N., Jang, Y., Mutha, S., Jordan, A., Pearson, B. & Townsend, T. G. RCRA toxicity characterization of discarded electronic devices. *Environ. Sci. Technol.* **40**, 2721–2726 (2006).

19 Klemm, D., Heublein, B., Fink, H.-P. & Bohn, A. Cellulose: fascinating biopolymer and sustainable raw material. *Angew. Chem. Int. Ed.* **44**, 3358–3393 (2005).

20 Pérez, J., Muñoz-Dorado, J., de la Rubia, T. & Martínez, J. Biodegradation and biological treatments of cellulose, hemicellulose and lignin: an overview. *Int. Microbiol. Off. J. Span. Soc. Microbiol.* **5**, 53–63 (2002).

21 Nishino, T., Matsuda, I. & Hirao, K. All-cellulose composite. *Macromolecules* **37**, 7683–7687 (2004).

22 Sakurada, I., Nukushina, Y. & Ito, T. Experimental determination of the elastic modulus of crystalline regions in oriented polymers. *J. Polym. Sci.* **57**, 651–660 (1962).

23 Yu, G., Xie, X., Pan, L., Bao, Z. & Cui, Y. Hybrid nanostructured materials for high-performance electrochemical capacitors. *Nano Energy* **2**, 213–234 (2013).

24 Yu, G., Hu, L., Vosgueritchian, M., Wang, H., Xie, X., McDonough, J. R., Cui, X., Cui, Y. & Bao, Z. Solution-processed graphene/MnO2 nanostructured textiles for high-performance electrochemical capacitors. *Nano Lett.* **11**, 2905–2911 (2011).

25 Kang, W., Yan, C., Foo, C. Y. & Lee, P. S. Foldable electrochromics enabled by nanopaper transfer method. *Adv. Funct. Mater.* **25**, 4203–4210 (2015).

26 Jung, Y., Chang, T., Zhang, H., Yao, C., Zheng, Q., Yang, V. W., Mi, H., Kim, M., Cho, S., Park, D., Jiang, H., Lee, J., Qiu, Y., Zhou, W., Cai, Z., Gong, S. & Ma, Z. High-performance green flexible electronics based on biodegradable cellulose nanofibril paper. *Nat. Commun.* **6**, 7170 (2015).

27 Saheb, D. N. & Jog, J. P. Natural fiber polymer composites: a review. *Adv. Polym. Technol.* **18**, 351–363 (1999).

28 Zhu, H., Parvinian, S., Preston, C., Vaaland, O., Ruan, Z. & Hu, L. Transparent nanopaper with tailored optical properties. *Nanoscale* **5**, 3787–3792 (2013).

29 Saito, T., Hirota, M., Tamura, N., Kimura, S., Fukuzumi, H., Heux, L. & Isogai, A. Individualization of nano-sized plant cellulose fibrils by direct surface carboxylation using TEMPO catalyst under neutral conditions. *Biomacromolecules* **10**, 1992–1996 (2009).

30 Unsal, O., Candan, Z. & Korkut, S. Wettability and roughness characteristics of modified wood boards using a hot-press. *Ind. Crops Prod.* **34**, 1455–1457 (2011).

31 Nogi, M., Iwamoto, S., Nakagaito, A. N. & Yano, H. Optically transparent nanofiber paper. *Adv. Mater.* **21**, 1595–1598 (2009).

32 Vosgueritchian, M., Lipomi, D. J. & Bao, Z. Highly conductive and transparent PEDOT: PSS films with a fluorosurfactant for stretchable and flexible transparent electrodes. *Adv. Funct. Mater.* **22**, 421–428 (2012).

33 Hu, L., Kim, H. S., Lee, J.-Y., Peumans, P. & Cui, Y. Scalable coating and properties of transparent, flexible, silver nanowire electrodes. *ACS Nano* **4**, 2955–2963 (2010).

34 Pengtao, J., Ji, W., Zeng, Q., Li, D., Qu, S., Wang, J. & Zhang, D. Vacuum-free transparent quantum dot light-emitting diodes with silver nanowire cathode. *Sci. Rep.* **5**, 12499 (2015).

35 Kim, K. S., Zhao, Y., Jang, H., Lee, S. Y., Kim, J. M., Kim, K. S., Ahn, J. A., Kim, P., Choi, J. Y. & Hong, B. H.. Large-scale pattern growth of graphene films for stretchable transparent electrodes. *Nature* **457**, 706–710 (2009).

36 Lee, M. S., Lee, K., Kim, S. Y, Lee, H., Park, J., Choi, K. H., Kim, H. K., Kim, D. G., Lee, D. Y., Nam, S. & Park, J. U. High-performance, transparent, and stretchable electrodes using graphene–metal nanowire hybrid structures. *Nano Lett.* **13**, 2814–2821 (2013).

37 Lee, Y., Kim, T. S., Min, S. Y., Xu, W., Jeong, S. H., Seo, H. K. & Lee, T. W. Individually position-addressable metal-nanofiber electrodes for large-area electronics. *Adv. Mater.* **26**, 8010–8016 (2014).

38 Min, S. Y., Kim, T. S., Kim, B. J., Cho, H., Noh, Y. Y., Yang, H., Cho, J. H. & Lee, T. W. Large-scale organic nanowire lithography and electronics. *Nat. Commun.* **4**, 1773 (2013).

39 Kim, D. H., Song, J., Choi, W. M., Kim, H. S., Kim, R. H., Liu, Z., Huang, Y. Y., Hwang, K. C., Zhang, Y. W. & Rogers, J. A. Materials and noncoplanar mesh designs for integrated circuits with linear elastic responses to extreme mechanical deformations. *Proc. Natl Acad. Sci.* **105**, 18675–18680 (2008).

40 Romeo, A., Liu, Q., Suo, Z. & Lacour, S. P. Elastomeric substrates with embedded stiff platforms for stretchable electronics. *Appl. Phys. Lett.* **102**, 131904 (2013).

This work is licensed under a Creative Commons Attribution 4.0 International License. The images or other third party material in this article are included in the article's Creative Commons license, unless indicated otherwise in the credit line; if the material is not included under the Creative Commons license, users will need to obtain permission from the license holder to reproduce the material. To view a copy of this license, visit http://creativecommons.org/licenses/by/4.0/

© The Author(s) 2016

Supplementary Information accompanies the paper on the NPG Asia Materials website (http://www.nature.com/am)